Analysis of Data Spectral Regrowth from Nonlinear Amplification

Frank Amoroso and Robert A. Monzingo

Abstract: **The regrowth of OQPSK power spectral sidelobes from AM/AM and AM/PM amplifier nonlinearity is analyzed. The time-domain expression for amplifier output shows how spectral regrowth will depend on the cubic coefficient of the Taylor's series of the amplifier nonlinearity as well as input amplitude ripple. Closed form spectrum calculations show that the spectral sidelobes produced by AM/PM take the same form as those produced by AM/AM. The rate of growth of AM/PM sidelobes is, however, not as great as for AM/AM.**

Index Terms: **Spectral Regrowth, AM/PM, AM/AM, OQPSK.**

I. INTRODUCTION

The representation of a nonlinear amplifier's saturation characteristic as a Taylor's series is well founded within the context of spectral analysis [1]. Previous studies [1] have concerned themselves with intermodulation products among simultaneous unmodulated sinusoidal inputs. The present discussion extends that mode of analysis to accommodate random digital data signal inputs. Here a bandlimited offset quadriphase shift keyed (OQPSK) signal passes through a soft saturating amplifier. The first stage of the present analysis treats spectral sidelobe regrowth from amplitude distortion (AM/AM) effects only. The extension to AM/PM conversion enters at a second stage of analysis.

In both stages of analysis the instantaneous input signal power level will at first be assumed small-to-moderate with a slight data-induced ripple in the carrier amplitude. The assumption of only slight ripple is a direct consequence of the assumption of OQPSK modulation. For example, the input might be a minimum-shift keyed (MSK) random data signal in which the classical baseband MSK signal has been low pass filtered prior to carrier modulation, so that the carrier amplitude no longer presents the perfectly constant value classically associated with MSK. It will then be shown that the results obtained for small-to-moderate power levels will also hold for hard limiting of a strictly bandlimited input.

II. INPUT AND OUTPUT SIGNAL REPRESENTATIONS

The input signal is assigned the usual passband expression

$$s(t) = \alpha(t)\cos[2\pi f_c t + \phi(t)], \tag{1}$$

Manuscript received December 7, 1998; approved for publication by Giuseppe Caire, Division I Editor, March 11,1999.

F. Amoroso is at 271-D West Alton Street, Santa Ana, CA 92707 USA.

R. A. Monzingo is at 624 Twenty-Sixth Street, Manhattan Beach, CA 90266 USA.

where $\alpha(t)$ is the non-negative input amplitude, $\phi(t)$ represents input phase, and f_c is the carrier radio frequency. The complex baseband representation is

$$s(t) = \alpha(t)e^{j\phi(t)}. \tag{2}$$

Assume, as usual, that the amplifier's saturation is represented by a Taylor's series having only odd coefficients. (Classically, any even-numbered terms give rise only to frequency products near harmonics of f_c, which are rejected by the zonal passband characteristic typical of practical amplifiers.) The amplifier output is therefore expressed

$$r(t) = K_1 s(t) + K_3[s(t)]^3 + K_5[s(t)]^5 + \cdots, \tag{3}$$

where K_1 is further normalized to unity without loss of generality. The model in (3) will suffice for the analysis of AM/AM effects.

III. ANALYSIS OF AM/AM EFFECTS

The analysis of AM/AM power spectral sidelobe regrowth versus amplifier drive level proceeds temporarily in the realm of real passband signals, which include the modulating carrier. The following relationship will soon prove useful in dealing with the Taylor's series representation of the amplifier characteristic

$$s^3(t) = \alpha^3(t)\left\{.75\cos[2\pi f_c t + \phi(t)] + .25\cos[6\pi f_c t + 3\phi(t)]\right\}. \tag{4}$$

Now the rippling input signal amplitude $\alpha(t)$ will be assumed centered at its mean value α_0, with relatively small smooth variation $\delta_\alpha(t)$ above and below α_0,

$$\alpha(t) = \alpha_0[1 + \delta_\alpha(t)]. \tag{5}$$

(Note that $\delta_\alpha(t)$ is not at all related to the Dirac delta function.) The mean value of $\delta_\alpha(t)$ is, by definition, zero. That portion of $s^3(t)$ that falls in the vicinity of f_c, i.e. the portion that is passed by the zonal bandpass filter inherent to the amplifier, is readily shown to be

$$\hat{s}^3(t) = \alpha_0^2\left\{.75s(t) + 1.5\alpha_0\delta_\alpha(t)\cos[2\pi f_c t + \phi(t)]\right\}. \tag{6}$$

With (3) truncated at the cubic term in accordance with the assumption of small-to-moderate drive levels, and with higher order terms in $\delta_\alpha(t)$ deleted in accordance with the assumption of

small ripple, the complex baseband output is

$$\begin{aligned}\hat{r}(t) &= s(t) + K_3\hat{s}^3(t) \\ &= s(t) + K_3\alpha_0^2[.75s(t) + 1.5\alpha_0\delta_\alpha(t)e^{j\phi(t)}] \\ &= (1 + .75K_3\alpha_0^2)s(t) + 1.5K_3\alpha_0^3\delta_\alpha(t)e^{j\phi(t)}.\end{aligned} \tag{7}$$

(The reversion to complex baseband will serve the needs of numerical spectrum calculation.) The implications of (7) for the power spectral density of $\hat{r}(t)$ become evident on examination of the two terms in the right side. The first term is just a constant times $s(t)$, hence reflects the power spectral density of the amplifier input. The presence of (usually negative-valued) K_3 within that constant time reflects the overall saturation effect on output power level. Only the second term in the right side of (7) may therefore reflect the spectral sidelobe regrowth that results from nonlinear amplification. It is convenient to express the second term in the right side of (7) as the product of $1.5K_3\alpha_0^3$ times the *parasignal*

$$\Delta(t) = \delta_\alpha(t)e^{j\phi(t)}. \tag{8}$$

The spectrum of the parasignal will be called the *paraspectrum*. Now (7) suggests that the paraspectrum actually represents the analytical form of the regrowing spectral sidelobes, and that those sidelobes increase as α_0^3. Therefore if the input power level were increased by 6 dB the main lobe of the output spectrum would be expected to increase by very nearly 6 dB, (with the $.75K_3\alpha_0^2$ term accounted for), and the sidelobes would be expected to grow 18 dB. These relative rates of growth are, incidentally, entirely consistent with the rates of growth of third order intermodulation products when the input consists of a pair of unmodulated sinusoids. More rigorous interpretation of (7) will be given next in section IV.

IV. SPECTRA FOR SPECIFIC SIGNAL AND AMPLIFIER, AM/AM EFFECTS

For illustration of (7), the OQPSK data signal input to the saturating amplifier is based on the following "trapezoidal" data pulse [2] for both the I and Q channels

$$p_o(t) = \frac{\sin\frac{\pi}{2T}t}{\frac{\pi}{2T}t} \times \frac{\sin\frac{\pi}{4T}t}{\frac{\pi}{4T}t}, \tag{9}$$

where the descriptor "trapezoidal" refers to the shape of the Fourier transform of the pulse as shown in Fig. 1a. If the pulse were allowed to extend from time $-\infty$ to $+\infty$ then its Fourier transform would be a trapezoid, but in practice some time truncation is obviously dictated. For the present study the pulse is truncated to the time interval $(-4T, +4T)$ to facilitate closed form spectrum calculations via a Markov method [3], [4] of autocorrelation computation. The basic pulse is also subjected to windowing [5] (sometimes called tapering) to reduce the time-truncation sidelobes and thereby expose the sidelobe regrowth to clearer view. The windowed pulse, which is the data pulse used here, is given by

$$\begin{aligned}p_o(t) = &\frac{\sin\frac{\pi}{2T}t}{\frac{\pi}{2T}t} \times \frac{\sin\frac{\pi}{4T}t}{\frac{\pi}{4T}} \\ &\times [0.42 + 0.5\cos(\pi t/4T) + 0.08\cos(\pi t/2T)]\end{aligned} \tag{10}$$

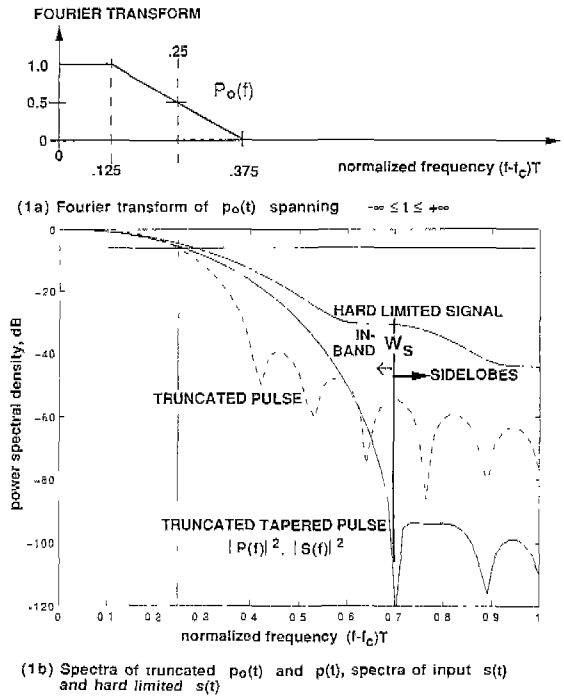

Fig. 1. Spectra underlying the data signal, all normalized to 0 dB at $(f - f_c)T = 0$.

for $0 \leq \mid t \mid \leq 4T$, and zero otherwise. The spectrum of $p(t)$, and therefore of the input data signal, is shown in Fig. 1b.

Note that, thanks to well-crafted windowing, the spectrum of $s(t)$ is very nearly bandlimited to the band designated W_s in Fig. 1b. All spectral components lying above W_s, whether from time truncation or nonlinear regrowth, are referred to as sidelobes. A further advantage of (10) is that it reduces the signal's RMS ripple δ_{rms} to just 10%.

Now the interpretation of (7) may be refined. Suppose that $s(t)$ is *perfectly* bandlimited to W_s. It becomes meaningful to partition both sides of (7) to those frequency components that lie below W_s versus those frequency components that lie above W_s. Since $s(t)$ is perfectly bandlimited to W_s it contains no components above W_s. That portion of (7) that lies above W_s becomes

$$\hat{r}(t)_\sigma = 1.5K_3\alpha_0^3\Delta(t)_\sigma, \tag{11}$$

where the subscript σ indicates "sidelobes". Thus, the quantity $\hat{r}(t)_\sigma$ represents that part of the amplifier output that appears as spectral sidelobes. The quantity $\Delta(t)_\sigma$ is that part of the parasignal that falls above W_s.

In simpler terms, the spectral sidelobes of $\hat{r}(t)$ are *identical in shape* to the paraspectrum. Again, the assumptions are that (i) the power level of $s(t)$ is small-to-moderate, so that the amplifier's saturation characteristic may be represented accurately by the linear and cubic terms of its Taylor's series representation, (ii) the input ripple is small, and that (iii) the input $s(t)$ is strictly bandlimited below some frequency W_s. The next step, by way of example, is to assign numerical value to the parameters of the amplifier saturation characteristic.

At passband the assumed amplifier will have an instantaneous

transfer characteristic, with the carrier included, of [6], [7]

$$y(u) = \sqrt{\frac{\pi}{2}}\,\mathrm{erf}\left[\frac{\sqrt{2u}}{2}\right], \quad \text{where} \quad \mathrm{erf}(x) \equiv \int_0^z \frac{2}{\sqrt{\pi}} e^{-z^2} dz. \tag{12}$$

Routine calculations show that for (12) the value of K_3 in the Taylor's series (3), is $-\frac{1}{6}$ (with K_1 normalized to unity). But before (12) can be employed in output power spectral density calculations the equivalent complex baseband nonlinear characteristic must be derived. Only then can the available Markov spectrum calculation be utilized, as such Markov programs become practical only at complex baseband.

At complex baseband, after output frequency components that fall outside the amplifier's zonal passband have been filtered away, the amplifier's nonlinear transfer characteristic becomes a complex function of $\alpha(t)$. The magnitude of that transfer characteristic is $Y[\alpha(t)]$, the Chebyshev transform [6], [7] of $y(u)$, and the amplifier is assumed phase-transparent during this purely AM/AM analysis. In the present instance [6], [7]

$$Y[\alpha(t)] = \alpha(t)\exp\left[\frac{-\alpha^2(t)}{4}\right]\left\{I_0\left[\frac{\alpha^2(t)}{4}\right] + I_1\left[\frac{\alpha^2(t)}{4}\right]\right\}, \tag{13}$$

where $I_0(z)$ and $I_1(z)$ are the usual modified Bessel functions, so that the complex baseband amplifier response becomes

$$r(t) = Y[\alpha(t)]e^{j\phi(t)}. \tag{14}$$

V. COMPUTED RESULTS

The power spectral densities (PSD) in the following figures are, as computed by the Markov program, precise probabilistic results, accurate to several decimal places. Fig. 2 shows the output PSD, $|R(f)|^2$ for drive levels $\alpha_0 = 0.2$, $\alpha_0 = 0.4$, and $\alpha_0 = 0.8$, all below the 1dB compression point of the amplifier. These results are based directly on (13) and depend on no Taylor's series approximations or assumptions on the percent ripple. The drive levels are sufficient to raise the power spectral sidelobes substantially above the time-truncation sidelobes of $p(t)$ over the frequency interval $0.7 \le |f| \le 1$. Hence there is no significant interaction between the nonlinear saturation sidelobes and the time truncation sidelobes. This is the critical frequency region for control of sidelobes, as most engineering specifications imply the most exacting control in this region.

The theory discussed in above suggests that the ordinate separation, in decibels, between the successive sidelobes should be three times that separating the drive levels, i.e. the highest and lowest sidelobes should be separated by 36 dB because the highest and lowest drive levels are separated by 12 dB. Careful inspection of Fig. 2 will show that the upper and lower sidelobe plots are, indeed, separated by 36 dB.

The implications of (7) are now explored through Fig. 3. The "estimated spectrum" is simply the sum of input power

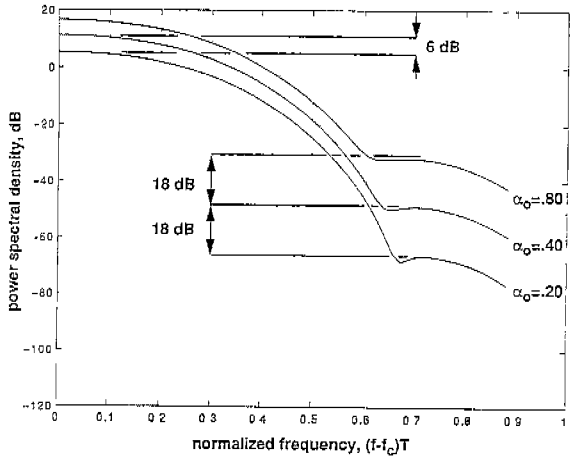

Fig. 2. Power amplifier output spectra for three drive levels 6 dB apart.

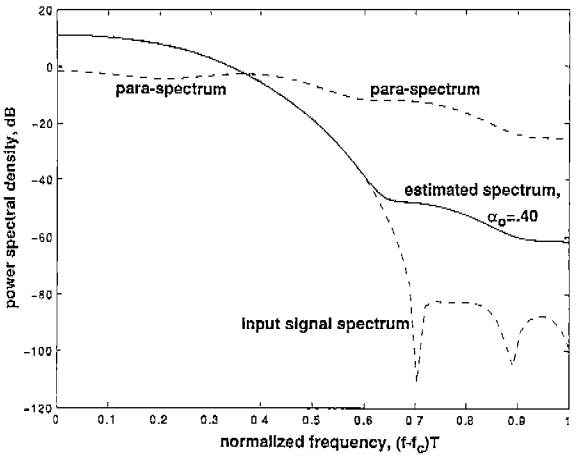

Fig. 3. Estimated power amplifier output spectrum for $\alpha_0 = .40$, based on the sum of input signal spectrum and paraspectrum.

spectral density, $|S(f)|^2$, plus the properly scaled paraspectrum $1.5K_3\alpha_0^3\Phi_\triangle(f)$ in accordance with (7). The paraspectrum $\Phi_\triangle(f)$ is the Fourier transform of the autocorrelation function $\phi_\triangle(\tau)$ of the parasignal. Shown for comparison are the underlying components $|S(f)|^2$ and $\Phi_\triangle(f)$. Note that since the scaled paraspectrum $1.5K_3\alpha_0^3\Phi_\triangle(f)$ is much smaller than the main spectral lobe, that main lobe is left virtually intact by the amplifier. Comparison of the estimated spectrum from Fig. 3 with the exact spectrum in Fig. 2 shows coincidence to within plotting accuracy for $\alpha_0 = 0.40$.

A further implication of (7) emerges from the consideration of bandpass hard limiting operation as illustrated in Fig. 4. The hard limiter output is, by definition, $s(t)/|s(t)|$, which equals $e^{j\phi(t)}$. Because $e^{j\phi(t)}$ can be expressed

$$e^{j\phi(t)} = [1 + \delta_\alpha(t)]e^{j\phi(t)} - \delta_\alpha(t)e^{j\phi(t)}. \tag{15}$$

The right side of (15) can be partitioned into those components that lie below W_s versus those that lie above W_s. By definition the expression $[1 + \delta_\alpha(t)]e^{j\phi(t)}$ is just equal to $s(t)$, which is bandlimited below W_s. That leaves $-\delta_\alpha(t)e^{j\phi(t)}$ alone to represent the frequency components that lie above W_s. In other

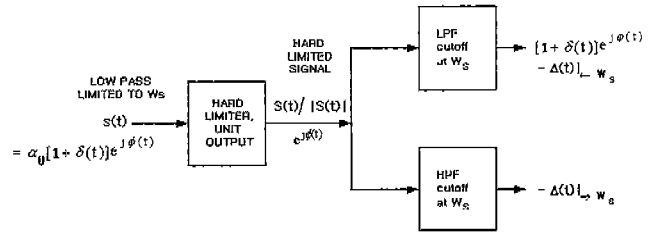

Fig. 4. Hard limited spectrum and paraspectum identical in sidelobe region.

words, when the amplifier is driven to hard limiting the sidelobes are, to within a sign change, given by $\delta_\alpha(t)e^{j\phi(t)} = \triangle(t)$, the parasignal, in the frequency band above W_s.

Returning to Fig. 1, the plot labeled "hard limited signal" clearly matches the paraspectrum as plotted in Fig. 3, at least for frequencies above W_s. This validates the arguments that flow out of (15) above. These arguments are free of any Taylor's series representation of the amplifier characteristic. They hold as long as $s(t)$ is strictly bandlimited.

VI. EXTENSION TO AM/PM EFFECTS

The problem to be addressed here is the extension of the above theory to the combination of AM/PM distortion and AM/AM distortion, wherein the AM/PM aspect of the amplifier characteristic can be approximated (over the restricted range of the OQPSK carrier amplitude ripple) by a linear proportionality between phase shift and instantaneous carrier ripple. The instantaneous AM/PM phase shift is therefore

$$\phi_\varepsilon(t) = \alpha_0 k_\phi \delta_\alpha(t), \tag{16}$$

where k_ϕ represents the AM/PM coefficient of the amplifier, with the result that (7), with AM/PM included, becomes

$$\hat{r}(t)e^{j\phi_\varepsilon(t)} = \hat{r}(t)e^{j\alpha_0 k_\phi \delta_\alpha(t)}. \tag{17}$$

The following sequence of approximations will reduce (17) to a more usable form. With the assumption of relatively small ripple it is useful to express the exponential as a power series

$$e^z = 1 + z + \frac{z^2}{2!} + \frac{z^3}{3!} + \cdots, \tag{18}$$

wherein only the first two terms need be retained. Thus

$$e^{j\alpha_0 k_\phi \delta_\alpha(t)} \approx 1 + j\alpha_0 k_\phi \delta_\alpha(t), \tag{19}$$

so that the amplifier output with the assumed AM/PM conversion becomes

$$\hat{r}(t)[1 + j\alpha_0 k_\phi \delta_\alpha(t)] = \hat{r}(t) + j\alpha_0 k_\phi \delta_\alpha(t)\hat{r}(t). \tag{20}$$

In other words, added to the output signal is a $\pi/2$ phase-shifted version of $r(t)\delta_\alpha(t)$ that is scaled down to the small size of $\alpha_0 k_\phi$.

Now the product $\alpha_0 k_\phi \delta_\alpha(t)\hat{r}(t)$ will be approximated for small $\delta_\alpha(t)$ by

$$\begin{aligned}&(1 + .75K_3\alpha_0^2)s(t)\alpha_0 k_\phi \delta_\alpha(t)\\ &= (1 + .75K_3\alpha_0^2)\alpha_0[1 + \delta_\alpha(t)]e^{j\phi(t)}\alpha_0 k_\phi \delta_\alpha(t)\end{aligned} \tag{21}$$

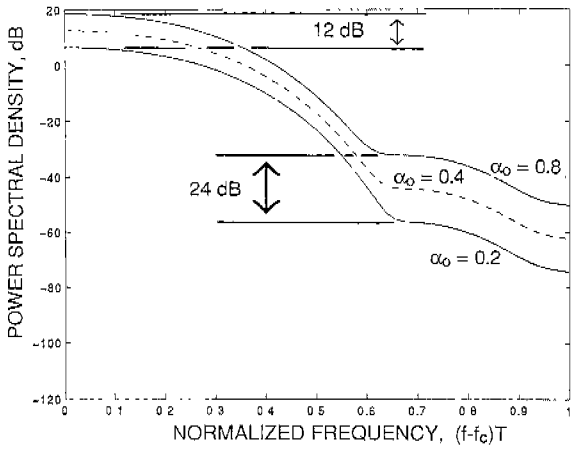

Fig. 5. Sidelobe regrowth, AM/PM effects only.

and when, owing to small ripple, terms in $\delta^2(t)$ are dropped the expression (21) reduces to

$$(1 + .75K_3\alpha_0^2)\alpha_0^2 k_\phi \delta_\alpha(t)e^{j\phi(t)} = (1 + .75K_3\alpha_0^2)\alpha_0^2 k_\phi \triangle(t), \tag{22}$$

wherein the final factor $\triangle(t)$ is, of course, the parasignal.

The upshot of (22) is that AM/PM conversion, under the stated assumptions on drive level and ripple, leads to the simple addition at the amplifier output of a scaled down $\pi/2$ phase-shifted version of the same parasignal form that is present from AM/AM conversion alone. Thus, the *combined* effect of AM/AM conversion and AM/PM conversion is the addition to the amplifier output of a properly scaled and phased version of the parasignal $\triangle(t)$.

This conclusion is now validated by Markov calculation of the spectrum of an OQPSK signal built on the assumed pulse (10) and the assumption that the AM/PM phase modulation is represented exactly by $e^{j\alpha_0 k_\phi \delta_\alpha(t)}$ as in (17). The amplitude characteristic of the amplifier has temporarily been assumed perfectly linear. Again, there is no reliance on power series approximations of the amplifier characteristic. The AM/PM coefficient k_ϕ is set to 0.115 radians/volt, the value that causes the pure AM/PM sidelobes to coincide with the previously computed pure AM/AM sidelobes at $\alpha_0 = 0.40$, a choice motivated purely for illustrative purposes. Fig. 5 shows the sidelobe regrowth from AM/PM alone for the same values of α_0 that underlie Fig. 2.

From Fig. 5 a salient feature of (22) becomes evident. Under the reasonable approximation that $.75K_3\alpha_0^2$ is small compared with unity, the AM/PM paraspectral sidelobes can be expected to grow as α_0^3 as in the case of AM/AM conversion. Note that the highest and lowest sidelobes in Fig. 5 are 24 dB apart, as compared with the 36 dB separation that was observed in Fig. 2. The shape of the regrown sidelobes is, of course, identical between Fig. 2 and Fig. 5.

Fig. 6 shows the combined effect of AM/AM and AM/PM conversion for the same values of α_0 that were used in Figs. 2 and 5. Again the calculation is exact, based directly on (13) and (16). Because the AM/AM sidelobes grow at a faster rate than

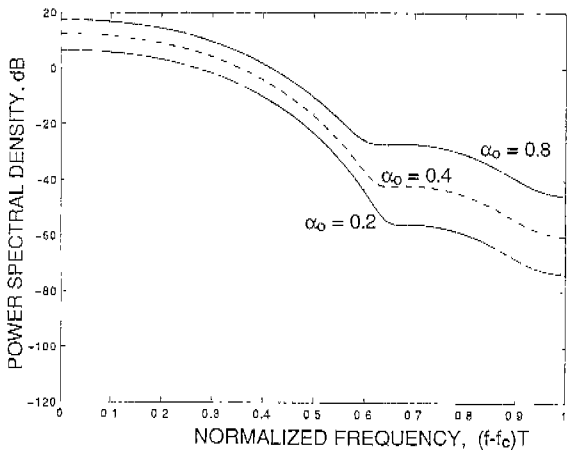

Fig. 6. Sidelobe regrowth, combined AM/AM and AM/PM.

the AM/PM sidelobes, the spacing is no longer uniform among sidelobes. The spacing between the upper and middle sidelobes is, as expected, slightly greater than between the middle and lower sidelobes.

VII. CONCLUSIONS

The present discussions have established the following relevant properties of the parasignal $\triangle(t)$, its autocorrelation function $\phi_{\triangle}(\tau)$, and the Fourier transform of $\phi_{\triangle}(\tau)$, here named the paraspectrum $\Phi_{\triangle}(f)$.

1. If $s(t)$ is bandlimited, then the spectral sidelobes from passband hard limiting are given precisely by the paraspectrum.
2. If $s(t)$ is bandlimited, and its amplitude ripple is relatively small, then the spectral sidelobes at small to medium input power levels (with AM/AM conversion only) are given to a close approximation by the paraspectrum. Those sidelobes grow as the cube of input power, while the output signal power itself remains substantially proportional to the power level of $s(t)$.
3. If AM/PM distortion is present and grow linearly with input signal amplitude, then the output sidelobes at small to medium power levels are again given to a very close approximation by the paraspectrum. The sidelobe levels from AM/PM grow as the square of input signal power. The AM/PM sidelobe component of the amplifier output is in quadrature with both $s(t)$ and the sidelobe components from AM/AM conversion.

Two previous works [8], [9] have demonstrated the performance of an AM/AM predistortion strategy based in the parasignal concept discussed above. The extension to a more comprehensive strategy that could combat AM/PM as well as AM/AM distortion would involve only simple, straightforward steps of generalization to deal with the quadrature paraspectral component generated by AM/PM distortion. Such a generalization is more properly the subject of a future discourse.

REFERENCES

[1] R. G. Sea, "An algebraic formula for amplitudes of intemodulation products involving an arbitrary number of frequencies," *Proc. IEEE*, vol. 56, no. 8, pp. 1388–1389, Aug. 1968.
[2] F. Amoroso and M. Montagnana, "Distortionless data transmission with minimum peak voltage," *IEEE Trans. Inform. Theory*, vol. IT-13, no. 3, pp. 470-477, July 1967.
[3] F. Amoroso, "The use of quasi-bandlimited pulses in MSK transmission," *IEEE Trans. Commun.*, vol. COM-27, no. 10, pp. 1616–1624, Oct. 1979.
[4] F. Amoroso and R. A. Monzingo, "Analysis of data spectral regrowth from nonlinear amplification," in *1997 IEEE International Conference on Personal Wireless Communications (ICPWC'97)*, Mumbai (formerly Bombay), India, 17-20 Dec. 1997, pp. 142–146.
[5] F. Harris, "On the use of windows for harmonic analysis with the discrete-Fourier transform," *Proc. IEEE*, vol. 66, no. 1, pp. 19–51, Jan. 1978.
[6] N. M. Blachman, "Detectors, bandpass nonlinearities, and their optimization: inversion of the Chebyshev transform," *IEEE Trans. Inform. Theory*, vol. IT-17, no. 4, pp. 398–404, July 1971.
[7] J. J. Spilker, *Digital Communications by Satellite*, Englewood Cliffs: Prentice-Hall, 1977.
[8] R. A. Monzingo and F. Amoroso, "Suppress spectral sidelobe regrowth with data signal predistortion," *Applied Microwve & Wireless*, vol. 10, no. 8, pp. 62 ff., Oct. 1998.
[9] F. Amoroso, "Spectral containment by predistortion of OQPSK signals," *Microwave Journal*, vol. 41, no. 10, pp. 22 ff., Oct. 1998.

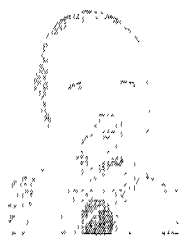

Frank Amoroso earned the B.S. and M.S. degrees in electrical engineering at Massachusetts Institute of Technology, Cambridge, in 1958, then pursued additional graduate studies at Purdue University of Turin, Italy.

His career in U.S. industry included such organizations as the Hughes Aircraft Company, the RCA David Sarnoff Research Laboratories, the Mitre Corporation, and the U.S. Army Signal Corps Laboratories at Fort Monmouth, NJ. IN 1989 he retired from industrial employment to begin a new career as private consultant to a number of industrial firms, including Lincom, Inc. of Los Angeles, CA.

Mr. Amoroso holds five U.S. patents, has published 30 papers in various archival quality journals, and has taught seminar courses at the George Washington University. On four occasions he served as session chairman and organizer for the *IEEE Conference on Military Communications* (MILCOM), and in September 1966 he served as organizer and chair for a session devoted exclusively to one of his own concepts, mitigation bandwidth at the *ISSSTA' 96* conference in Mainz, Germany. His accomplishments are recognized in the current edition of Marquis *who's who in America*.

Robert A. Monzingo holds a Sc.D. in systems and automatic control from Washington University, St. Louis, a M.S. in electrical engineering from the University of Arizona, Tucson, and a B.S.E.E. from Stanford University, Stanford, CA.

Currently, he is a Senior Scientist in the Adaptive Signal Processing Systems Division of the Raytheon Systems Company in Los Angeles, CA. Prior to joining the Sensors and Communications Division, he was associated with the Space and Communications Division of Hughes where he conducted system tradeoff studies for satellite payloads and modulation formats for satellite links.

Dr. Monzingo coauthored a book titled *Introduction to Adaptive Arrays*, and authored or coauthored numerous technical papers in estimation theory, adaptive antenna arrays, communication theory, and control theory.